Engineering and Technology Journal
Journal homepage: https://etj.uotechnology.edu.iq

Experimental and Numerical Flexural Properties of Sandwich Structure with Functionally Graded Porous Materials

Emad K. Njim [a*], **Sadeq H. Bakhi** [b], **Muhannad Al-Waily** [c]

[a,b] University of Technology-Iraq, Alsina'a street, 10066 Baghdad, Iraq.
[c] University of Kufa, Najaf, Iraq.
*Corresponding author Email: emad.njim@gmail.com

HIGHLIGHTS

- A novel of sandwich beam made of FG polymer porous core and homogenous skins.
- Flexural properties of FPGM sandwich beams.
- Effects of changing the core thickness and porosity parameters on the FGM beam.
- Used experimental work and the finite element method (FEM).
- FGPMs are crucial components of various engineering applications.

ARTICLE INFO

Handling editor: Muhsin J. Jweeg
Keywords:
Sandwich beam
Functionally graded porous materials
PLA core
Three-point Bending
FEA

ABSTRACT

Functionally graded porous materials (FGPMs) are porous structures with a porosity gradient distributed over the entire volume. They have many applications in the aerospace, marine, biomedical, automotive, and shipbuilding industries. High strength to weight and excellent energy absorption is the most important features that make these structures unique. In this paper, the flexural properties of simply-supported sandwich beams with functionally graded porous core under flexural load were evaluated experimentally and numerically based on various parameters. A three-point bending test for 3D printed sandwich specimens with porous metal core bonded with aluminum face sheets using various porosity parameters and core heights has been performed to measure the peak load and maximum deflection and explore the sandwich structure's strength. To validate the accuracy of the experimental solution, a finite element analysis (FEA) is carried out using ANSYS 2021 R1 software. Tests and FEM show that the sandwich beam behavior is closely related to porosity, power-law index, and FG porous metal core thicknesses. Experimental results indicated that at a porosity ratio of 10 %, FG core height 10 mm the maximum bending load was 573 N and maximum deflection 13.8 mm respectively. By increasing porosity to become 30% using the same geometrical parameters, the bending load was reduced by 15.4 % while the deflection exhibited a 1.4 % increase. The Numerical results for the three-point bending are compared with experimental measurements, showing a fair agreement with a maximum discrepancy of 15%.

1. Introduction

Functionally graded materials (FGMs) consist of mixtures of two or more ingredients, so the material properties continuously vary smoothly across the direction of beam thickness, which can reduce the residual stress and stress concentration factor in the laminated composite material [1]. FGMs are widely utilized in various important industries including but not limited to energy, automobile, defense, aerospace, and bioengineering [2, 3]. In the past few decades, the FG sandwich structure has been vastly employed in mechanical and civil engineering, due to its excellent characteristics such as high bending stiffness, low weight, high sound absorption, and damping performance [4, 5]. Generally, porosity is found in materials through the manufacturing stages or may be due to intentional formation. With the presence of pores, the rigidity of the whole structure is influenced, however, the total weight of the structures may be reduced [6]. The uniform arrangement of porosities through the thickness of these structures yields to sustain the performance of the structure or avert the occurring of stress concentration at the parts. Thus, the FG structures are fabricated from many alternative styles of FGM arrangement to take care of these characteristics. Therefore, functionally graded porous structures FGPMs have many essential applications in the engineering industry including bioengineering and aerospace. Most of the military equipment and aircraft are made from FG porous materials to reduce mass, increase heat resistance, and enhance overhaul performance [7, 8].

Many researchers have extensively studied the flexural behavior of honeycomb, foam, and composite materials sandwich structures [9-13]. FGMs with chemical composition, porosity, and microstructure gradients are being modified can reduce

http://doi.org/10.30684/etj.v40i1.2184
Received 25 May 2021; Accepted 20 June 2021; Available online 25 January 2022
2412-0758/University of Technology-Iraq, Baghdad, Iraq

damage caused by impact in sandwich structures with composites [14]. Recently, a lot of scientists worldwide studied the mechanical behavior of the FG porous sandwich structures. Ahmed Amine and Ashraf M Zen our presented new analytical solutions of bending analysis of FGM sandwich plate by employing various porosities distribution [15].

The bending problem of functionally graded beams with some important parameters includes volume fraction index, support and loading conditions, and beam configuration has been studied and introduced in Refs. [16–18]. As a consequence, the changing of the porosity density or pore size leads to generating functionally graded materials. Bending experiments of FGM structures have been also been studied in [19, 20]. A more comprehensive experimental study on the failure of the segmented FG sandwich beam using a three-point bending is presented by Ref. [21]. The bending behavior of sandwich composites using fiber-reinforced syntactic foam and syntactic foam core has also been studied in Refs. [22-24]. Simultaneously, the flexural properties were determined for the FG polymer Nanocomposite by conducting a three-point bending test loaded from neat and one wt.% side FG [25]. Volker Hardenacke et al. [26] carried out a combination of gradient porous material experiments and numerical design for multifunctional aerospace applications with functionally gradient materials as sandwich cores, using combined numerical and experimental methods. Amman Gag et al. [27] studied bending analysis of sandwich FGM beams consisting of ceramic skins, and exponentially varying FGM core using finite element analysis. They conducted a detailed study employing the power and sigmoidal law representation of the FGM beam. Lin Jing [28] conducted various experiments to study the effect of low-speed impact on FG beams response under different values of energies. The multi-objective design optimization of the sandwich beam was carried out. The results of the simulation show that the percentage of core absorbed energy decreases as the impact energy increases. A. Seyedkanani et al. [29] conducted different flexural tests on 3D printed samples to examine designs of FGM practicality for improving characteristics of lightweight structures. The experimental results are verified by FEA. Three-point bending and indentation tests are commonly used to calibrate mechanical models of homogeneous materials. The parameter estimation performed by this test is suitable for relatively large FGM layer thickness. It involves the phase distribution transverse to the sample and its fracture characteristics, particularly mechanical properties and absorbed energy of the cracked structure [30]. Czechowski L [31] studied the mechanical behavior of FGM samples, consisting of WC and Nicer, as well as a few Co. The flexural test is conducted to check the investigate proper parts proportions used on the bending stiffness and overall strength. Furthermore, to verify the experimental results, a micro-indentation technique simulates samples under similar loads. J. Zhou et al. [32] performed a low-speed impact test on a sandwich structure based on a core made of foams of various densities. Although many researchers in the literature have been investigated flexural properties in FG sandwich beams, but none of them conducted an experimental study with FG porous sandwich structures.

In this paper, a novel FG porous sandwich beam and homogenous skins are introduced and studied using flexural analysis to investigate the porosity influences and material gradation, on the bending behavior of porous FG beams having a variety of constituent's stiffness through their thickness. The experimental program is conducted to investigate the flexure tests on flat sandwich beams with porosities based on various parameters (core height, porosity parameter, and power-law index) to determine the sandwich flexural stiffness, the core shear strength, and deflections. A numerical method using FEA was used to validate the experimental results. The paper is organized as follows: the theoretical investigation of the FG structure is presented in section 2. Section 3 briefly offers the experimental tests of the three-point bending test. In section 4 verification study using FEA is presented. Results, of the flexural test of the FG sandwich beam with porosity with many beneficial discussions, are given in section 5. Furthermore, the paper also explores, in section 6 a few crucial conclusions on the flexural behaviors of FG sandwich beam with even distribution of porosities and good suggestions for future work.

2. Theoretical Investigation

In most of the previous works found in literature, the FGM structure (plate, beam, shell…, etc.) is assumed to be made of two-phase materials, (for example ceramic and metal). According to the power-law homogenization rule [33], the volume fraction of constituent 1 is can be represented in the following form

$$V_1(z) = \left(\frac{1}{2} + \frac{z}{h}\right)^k \tag{1}$$

where h is the total height of the FG cross-section structure, k is the power-law variation index, in which $k \in [0\ \infty)$. Thus $V_1 = 0$ at the lower surface ($z = -h/2$) and $V_1 = 1$ at the upper surface ($z = h/2$) of the FG part. According to the rule of mixtures, the total constituent volume fraction across the FG thickness is expressed as

$$V_1(z) + V_2(z) = 1 \tag{2}$$

where V_2 is the volume fractions of constituent 2, thus, the effective material property of an FGM using Eqs. (1) and (2) may be found

$$\emptyset(z) = \emptyset_1 V_1 + \emptyset_1 V_1 \tag{3}$$

Where ∅1 and ∅2 are the material properties of mixture constituents of the FG part, respectively. For the FGM structure with even porosity distribution throughout the thickness of the structure ($\beta < 1$), the material characteristics of the FGM structure with even distribution of pores may be given, as [35]:

$$\emptyset(z) = \emptyset_2 + (\emptyset_1 - \emptyset_2)\left(\frac{z}{h} + \frac{1}{2}\right)^k - (\emptyset_1 + \emptyset_2)\frac{\beta}{2} \quad (4)$$

The originality of the current work is related to developing a new mathematical formulation using the FG core of sandwich structure made up of only one phase metal with porosity changes through-thickness direction. Thus, the mechanical properties of the FG structure are given by:

$$V_p(z) = V_m - V_m\beta\left(\frac{z}{h} + \frac{1}{2}\right)^k \quad (5)$$

Where, V_m is the volume fraction of homogenous metal, while V_p volume fraction of porous metal, respectively. This new concept can be examined, for the k=0, $V_p(z) = (V_m - V_m\beta)$, while for, $k = \infty$, $V_p = V_m = 1$. Therefore, the new representation of the mechanical properties of FG structure can be expressed as:

$$\emptyset(z) = \emptyset_m - \emptyset_m\beta\left(\frac{z}{h} + \frac{1}{2}\right)^k \quad (6)$$

In the case of the homogenous core (β = 0), whereas the elastic modulus (E), material density (ρ), and the Poisson's ratio (ν) equations may be introduced as follows:

$$E(z) = E_m - E_m\beta\left(\frac{z}{h} + \frac{1}{2}\right)^k \quad (7)$$

$$\rho(z) = \rho_m - \rho_m\beta\left(\frac{z}{h} + \frac{1}{2}\right)^k \quad (8)$$

$$\nu(z) = \nu_m - \nu_m\beta\left(\frac{z}{h} + \frac{1}{2}\right)^k \quad (9)$$

Figure 1 shows the volume fraction relationship with the thickness ratio, while Figure 2 shows the material performance curve for the imperfect FGM structure when the porosity is 10% using the Ease. (4-7).

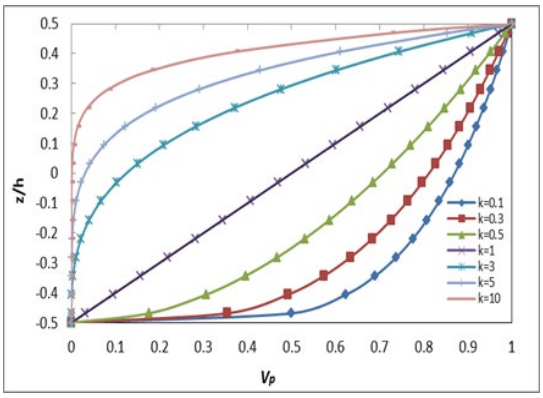

Figure 1: Volume fraction versus thickness

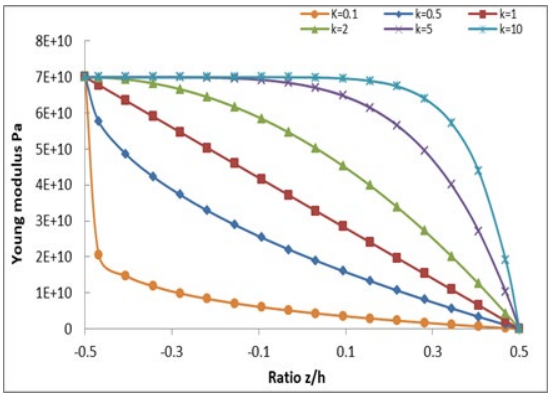

Figure 2: Young modulus versus thickness

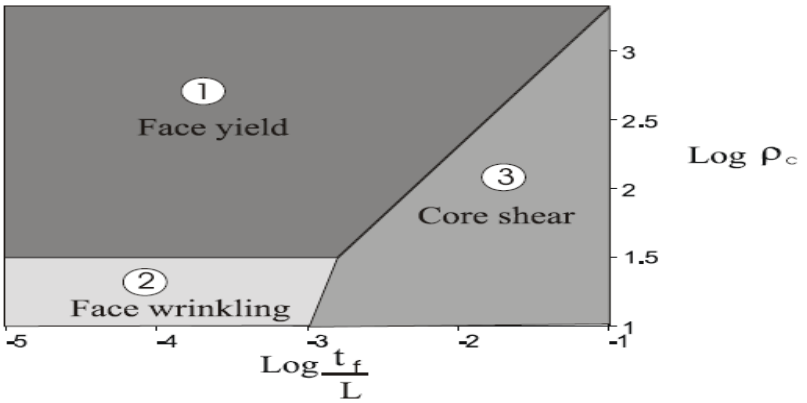

Figure 3: Three-point bending failure mode map for a sandwich beam having aluminium skins and FG core [36]

2.1 The failure mode of functionally graded sandwich beam with porous metal

According to the failure map shown in Fig.3, the failure modes and their critical loads of FG sandwich beams can be represented in five failure categories in flexure, including (1) Skin yielding; (2) Skin wrinkling; (3) failure by core shear; (4) Indentation of the core; (5) The adhesive bond failure [36]. In a 3-point bending test, the total deformation (δ) at beam midspan may be obtained by using the following equation [21],

$$\delta = \delta_b + \delta_s = \frac{Pl^3}{48(EI)_{eq}} + \frac{Pl}{4(AG)_{eq}} \tag{10}$$

Where P is the bending load, l: span, a: area of the core, and G is the shear modulus. Consequently, the total strength of the core and skins is given by

$$(EI)_{eq} = \left[E_f \left(\frac{bt^3}{12} + (bt)\, d_u{}^2\right) + E_f \left(\frac{bt^3}{12} + (bt)\, d_1{}^2\right) \right] + \sum E_i \left(\frac{b\, c_i{}^3}{12} + (bc_i)\, d_i{}^2\right) \tag{11}$$

And that the equivalent shear rigidity

$$(AG)_{eq} = \frac{bd^2 G_c}{c} \tag{12}$$

The subscript c and b refer to the core thickness and the beam's width, respectively. Furthermore, the subscript d is the distance of the centroid between the upper and lower skins; when d ≈ tic, Eq. 12 is reduced to

$$(AG)_{eq} = bdG_c \tag{13}$$

The bond failure type represented by the lower limit force is given as:

$$P_{bf} = 4bc_{\mathrm{i}} \left(\frac{t}{l}\right) \sqrt{\frac{SE_{\mathrm{f}}}{t}} \tag{14}$$

Where ci is the thicknesses of each core layer i, t is face sheet thickness, If is face-sheets elastic moduli and S is the rate of released strain energy which is given by:

$$S = \frac{M^2}{2b(EI)_{eq}} \tag{15}$$

The maximum bending moment M is calculated as $\mathrm{M} = \frac{\mathrm{Pl}}{4}$

3. Experimental Work

3.1 The material used and specimen's preparation

3D printing is a modern manufacturing technology that uses an additional process that deals with a 3D model of an object generated by CAD software or a scan of an existing object. The file format of the model used must be compatible with printer software such as STL (stereolithography) [37]. During this technique, the metal rope or filament is subjected to a heating process inside the head of the printer and melts. The molten batch is discharged through the nozzle due to passing the wire via the nozzle. Generally, objects are created by continuous material layers depositing in a molten state during the feeding process [38]. The bench on which the workpiece is mounted moves downward in the z-direction. Therefore, an accurate 3D entity will be created after a certain period, which is the same as the designed model. Polytrophic Lattice Acid (PLA) is a major biomaterial source for many medical applications [39], and it is the most commonly used material for manufacturing objects through 3D printing. It has a suitable temperature to be melted at some stage in the printing process, which leads to keeping the shape of the produced piece as its original design. Due to its features, 3D printing can produce complex shapes using fewer materials than traditional manufacturing techniques. 3D printing covers many forms of technologies and materials because almost all industries can employ 3D printing. It must be regarded as a cluster of different industries with many different applications, such as dental products, glasses, building scale models, prosthetics....., etc. One of the main goals of this study is to design and generate a distribution pattern of porosity in functionally graded cores. These distribution arrangements should follow the power-law distribution of volume fractions. To describe the distribution pattern, PLA samples with porosity are designed using the Solid Works program, then save the required model's geometry as a (.stl) file, and then use it to manufacture the sample through the CR-10 Max 3D printer as shown in Figure 4. The Aluminum alloy (AA6061-T6) plate, used for manufacturing automotive and aircraft structures is used in fabricating skins of the sandwich beam. Faces having 0.5 mm thickness were bonded to FG cores with various porosity distributions along thickness to form sandwich beams, using the SMX Hybrid polymer adhesive, with a high-quality, cured 30 minutes at 25° C under constant pressure, as shown in Figure 5. The chemical composition analysis of the aluminum alloy (AA6061-T6) was analyzed according to ASTM E1251-94; the results are given in Table 1. The specimens are manufactured at local markets and the dimension was fixed at (230 mm×

45mm) according to the ASTM standard C393. The geometrical properties of sandwich specimens used in experiments are listed in Table 2.

Table 1: Chemical composition of Aluminum alloys (AA6061-T6), in % by mass [40]

Element	Mn	Mg	Fe	Si	Cu	Cr	Zn	Ti	Al
Measured	1.16	0.856	0.58	0.437	0.139	0.039	0.008	0.229	Bal.
Standard	< 0.15	0.8-1.2	< 0.7	0.4-0.8	0.1-0.4	< 0.25	< 0.15	0.04-0.35	Bal.

Table 2: The dimensions of sandwich specimens

Specimen No.	Porosity (Beta)	Power-law Index (k)	Dimension of specimen (mm)	FG core height (mm)	Face sheet thickness (mm)
1	0	1	230 x 45	10	0.5
2	0	1	230 x 45	15	0.5
3	0	1	230 x 45	20	0.5
4	0	1	230 x 45	25	0.5
5	0.1	1	230 x 45	10	0.5
6	0.1	1	230 x 45	15	0.5
7	0.1	1	230 x 45	20	0.5
8	0.1	1	230 x 45	25	0.5
9	0.3	1	230 x 45	10	0.5
10	0.3	1	230 x 45	15	0.5
11	0.3	1	230 x 45	20	0.5
12	0.3	1	230 x 45	25	0.5

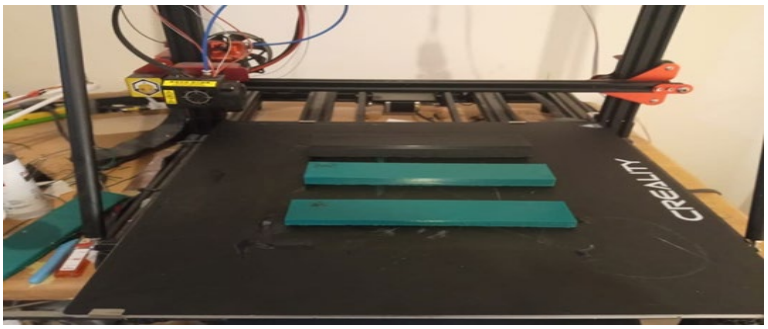

Figure 4: Manufacturing FG specimens using 3 D printing

3.2 Experimental setup

A three-point bending test is usually used to study sandwich panels' impact resistance and evaluate the bending performance. It gives the sandwich flexural strength and stiffness and core shear modulus of all types of materials and products [41]. A roller applies the load with a diameter (5mm) per the ASTM C393-00 [42] standard recommendations. The crosshead speed is kept constant and selected as (4mm/sec) using a simply supported rig. A transducer, deflect meter, or dial gauge can be used to measure the misspent deflection. By applying the load at the center of the specimen, the displacement was recorded on a PC; hence load-deflection curves can be generated to determine the sandwich stiffness and core shear modulus. Three specimens for each core height, with a total of twelve FG sandwich specimens for each porosity parameter value, were tested by a three-point bending device (universal device). Figure 6 depicts the three-point bending test schematic, while Figure 7 shows the experimental setup for the FG core beam.

4. Numerical Investigation

The Finite Element Modeling (FEM) is carried out to check the accuracy of numerical results with those obtained throughout three-point bending experiments. In this work, the commercial ANSYS software program 2020 R2 is executed to analyze the bending analysis of the sandwich beam. By using 8-node brick elements SOLID 45 type, the core of the beam model is generated, while the face sheets of the beams are constructed employing SHELL99 composite element type as shown in figure (8) [43,44]. A precision mesh study was employed and the corresponding boundary conditions are applied. The material characteristics used in the FE simulation are calculated using Equations (6-8), then introduced into the engineering library view of ANSYS. The general mechanical properties for the Aluminum skins and the PLA core are given in Table 3 [39, 40, and 45]. The bending load, total deformation, and misspent deflection of the FGPMs sandwich beam under static structural analysis are obtained based on various parameters. Furthermore, the flexural strength and the energy absorption of the FG

sandwich beam with two porosity coefficients (Beta= 10% and 20%), gradient exponent (k=1), and different core heights (10-25 mm) are determined.

Figure 5: FG sandwich specimens with porous metal core

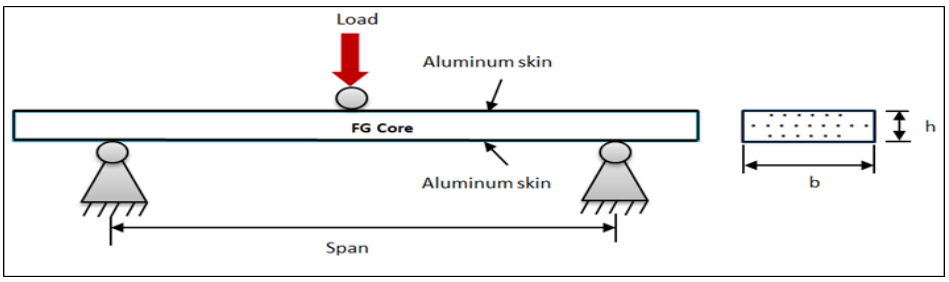

Figure 6: Three-point bending test configuration

Table 3: Mechanical properties of Aluminum alloys (AA6061-T6)

Property	Porous core (PLA)	Skins (Al)
Modulus of Elasticity (GPa)	2.4	70
Mass density (Kg/m3)	1360	2702
Poisson's ratio	0.4	0.3
Yield Stress (MPa)	70	276
Tensile Stress (MPa)	60	310

Figure 7: Experimental setup for the FG core sandwich beam

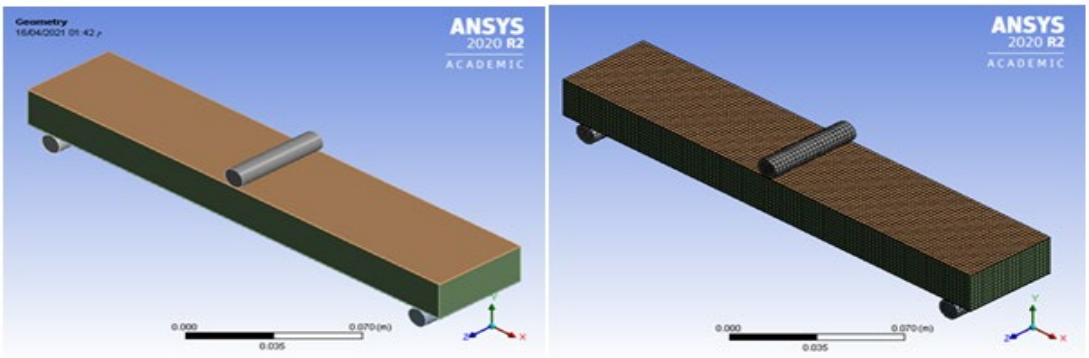

Figure 8: A 3D model of FG beam with mesh

Table 4: The numerical and experimental maximum bending load (N)

Porosity (Beta)	Power-law Index (k)	FG core height (mm)	Exp.	Num.	Discrepancy %
0.1	1	10	573	670	14.47
0.1	1	15	1140	1327	14.09
0.1	1	20	2200	2445	10.02
0.1	1	25	3830	4197	8.74
0.3	1	10	485	570	14.91
0.3	1	15	967	1100	12.09
0.3	1	20	1850	1935	4.39
0.3	1	25	3425	3650	6.16

Table 5: The numerical and experimental maximum bending deflection(mm)

Porosity	Power-law index	FG core height (mm)	Exp.	Num.	Discrepancy %
0.1	1	10	13.8	12.45	9.78
0.1	1	15	11.8	10.75	8.89
0.1	1	20	9.56	8.72	8.78
0.1	1	25	7.96	7.67	3.64
0.3	1	10	14	12.65	9.64
0.3	1	15	11	10.75	2.27
0.3	1	20	8.65	7.94	8.21
0.3	1	25	5.9	5.58	5.42

5. Results

Figures 9-12 show the experimental results of the load-displacement curves under a three-point bending condition of various samples of the simply supported porous functionally graded sandwich beams using different PLA core heights (0.010, 0.015, 0.020, and 0.025) m. Samples with two porosity parameters (Beta = 0.1 and 0.3), gradient index (k=1), and skins having a thickness of 0.5 mm each are examined using a Universal testing machine (Tinnitus Olsen H50KT apparatus). The experimental results include the maximum bending load and maximum total deflection at the mid-span of beams is obtained by utilizing the PC of the testing instrument. The numerical approach using ANSYS software is employed to validate the results due to experiments. As shown in Table 4 and Table 5, respectively. According to these tables, it can be concluded that the maximum difference in bending load does not exceed 15%, and the maximum difference in deflection does not exceed 13%. A possible source of error is mainly the adhesive material quality between the skin and the FG core in the sandwich sample, while the FEA solution is obtained based on the assumption of the perfect contact between skins and core of the FG sandwich beam. In addition, noise and system errors also determine the accuracy and reliability of the experimental static analysis. However, the most significant observations noticed from the configuration of the defective specimens throughout the experiments, are the most common reason for failure observed in the sandwich beam was the face-sheet yielding, as well as the possible deformation of FG core due to shear, will initiate and develop at the PLA core layers with a high porosity ratio. This reality is with a settlement of the failure mode map proven in Fig. 3, and what's concluded by Avila in Ref. [21].

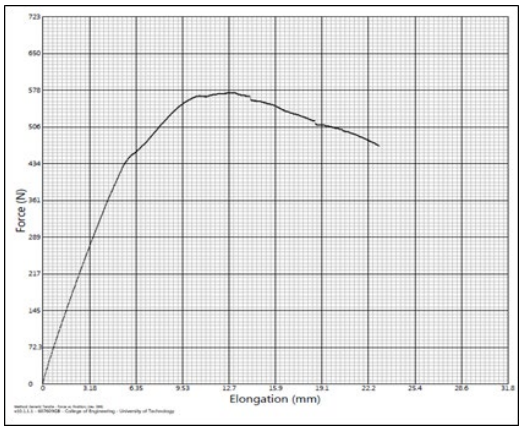

Figure 9: Displacement against force-sample 1

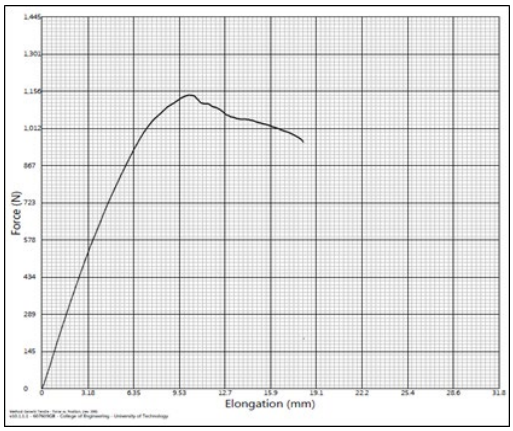

Figure 10: Displacement against force-sample 2

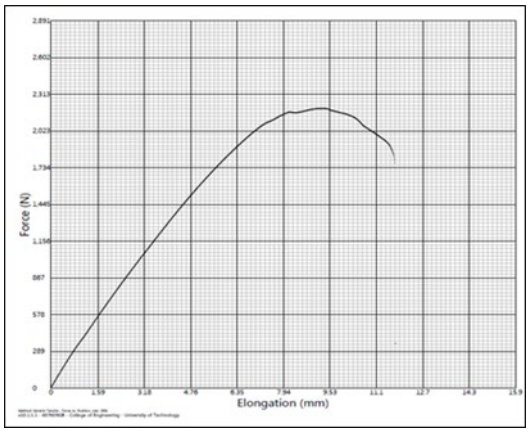

Figure 11: Displacement against force-sample 3

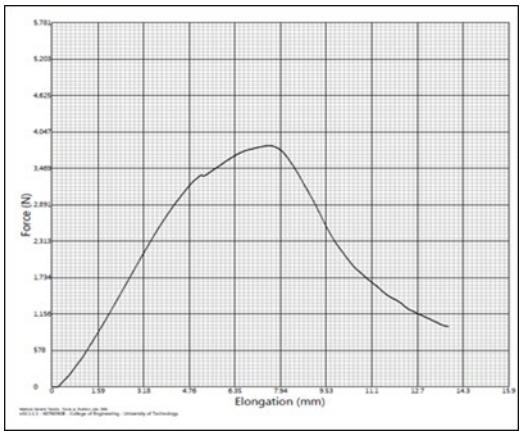

Figure 12: Displacement against force-sample 4

6. Conclusions

The lightweight of functionally graded materials (FGMs) and their outstanding energy absorption characteristics make them the most attractive, and popular in an aerospace application. In this paper flexural strength and stiffness of functionally graded beams with porous metal are investigated. Also, the present contribution relates to the combined experiment and numerical design of the FGM sandwich structure. From the research results the conclusion statement can be summarized as follows:

1) The variation of slenderness ratio L/h from (20.9 to 8.85) yields to increase the experimental bending load by 3.257 KN at porosity ratio (Beta 10%) and power-law index (k=1), while at porosity ratio (Beta 30 %) and same power-law index, the increase will be 2.94 KN.
2) The significant decrease in the porosity positively affects the bending stiffness and ultimate load of the sandwich FG sandwich beams. As the porosity coefficient decreases, the bending stiffness is improved, and the mid-span displacement is increased.
3) The flexural behavior of FG sandwich structures has been explored experimentally and numerically. According to the experimental research results, the FG beam fails under the bending load, and suddenly, brittle failure occurs.
4) The significant increase in bending stiffness due to the sandwich arrangement indicates that a FGPMs sandwich beam is applied to the outermost surface to withstand tensile and compressive loads.
5) It is evident from tables and graphs that there is a fair convergence between both experimental and Andy's analysis, where the maximum error percentage found no more than 15 % in bending and 10 % in deflection measurement, which indicates that a 3D printing method can use to manufacture good FGPMs samples.
6) A combination of numerical and experimental methods can design and optimize functionally graded sandwich cores. Their characteristics and performance will determine the required applications and comply with multifunctional requirements.

For future works, it is suggested to perform theoretical analysis according to the details of the above mathematical formulation. As well as it is preferred to develop optimization techniques using the design of experiments (DOE) and response surface method (RSM) to identify the optimized values of the beam dimensions, bending load, strain energy, and deflection.

Acknowledgment

The experimental work of this study is partially supported by the strength of the materials laboratory- University of Technology- Mechanical Engineering Department. Thanks to Eng. Zainab for the experimental assistance.

Nomenclatures

1. $V_1(z)$: Volume fractions of the first constituent
2. h: Core height (M)
3. k: Power-law index
4. V_2 (z): Volume fractions of the second constituent
5. Φ(z): Material property of the functionally graded structure
6. V_m: Volume fraction of homogenous metal
7. V_p: Volume fraction of porous metal
8. E(z): Young's modulus (MPa)
9. ρ (z): Density of the functionally graded structure (Kg/m^3)
10. ρ_m: Density of the homogenous metal (Kg/m^3)
11. P: Applied load (N)
12. l: the distance between supports (m)

13. A: Area (m^2)
14. G: Shear modulus (GPa)
15. (EI)eq: Flexural rigidity (N. m^2)
16. (AG)eq: Equivalent modulus of shear rigidity (N)
17. G_c: Shear modulus of core (MPa)
18. c: Core thickness (m)
19. b: Beam's width(m)
20. E_f: Face-sheets elastic moduli(MPa)
21. P_{bf}: Lower limit force (N)
22. S: Strain energy release rate (J)
23. M: The maximum bending moment at the mid-span (N. m)

Greek Symbols

1. β:Porosity parameter
2. δ: the deflection (m)
3. ν(z): Poisson's ratio the functionally graded structure

Abbreviations:

1. FGM: Functionally graded materials
2. FGPMs: Functionally graded porous materials
3. ASTM: American society for testing and materials
4. FEA: Finite Element Analysis
5. FEM: Finite Element Modeling
6. PLA: Polytrophic Lattice Acid
7. CAD: Computer-aided design

Author contribution

All authors contributed equally to this work.

Funding

This research received no specific grant from any funding agency in the public, commercial, or not-for-profit sectors.

Data availability statement

The data that support the findings of this study are available on request from the corresponding author.

Conflicts of interest

The authors declare that there is no conflict of interest.

References

[1] E. K. Njim, M. Al-Waily, S. H. Bakhy, A Critical Review of Recent Research of Free Vibration and Stability of Functionally Graded Materials of Sandwich Plate, IOP. Conf. Ser. Mater. Sci. Eng., 1094 (2021) . https://doi.org/10.1088/1757-899X/1094/1/012081

[2] M. Naebe , K. Shirvanimoghaddam, Functionally graded materials: A review of fabrication and properties, Appl. Mater. Today, 5 (2016) 223–245. https://doi.org/10.1016/j.apmt.2016.10.001

[3] D. K. Jha, T. Kant, R. K. Singh, A critical review of recent research on functionally graded plates, Compos. Struct., 96 (2013) 833–849. https://doi.org/10.1016/j.compstruct.2012.09.001

[4] H. Lazreg, H. A. Atmane, T. Abdelouahed, M. Ismail, E. Bedia, Free vibration of functionally graded sandwich plates using four-variable refined plate theory, Appl. Math. Mech. Engl. Ed., 32 (2011) 925–942. https://doi.10.1007/s10483-011-1470-9

[5] Y. Kiani, E. Bagherizadeh , M. R. Eslami, Thermal and mechanical buckling of sandwich plates with FGM face sheets resting on the Pasternak elastic foundation, Proc. Inst. Mech. Eng, Part C: J. Mec. Eng. Sci., 226 (2011) 32-41.

[6] T. Anderson, A 3-d elasticity solution for a sandwich composite with functionally graded core subjected to transverse loading by a rigid sphere, Compos. Struct, 60 (2003) 265-274. https://doi.org/10.1016/S0263-8223(03)00013-8

[7] A. Shahistha, B. Varghese, A. Baby, A review on functionally graded materials, Int. J. Eng. Sci., 3 (2014) 90-101.

[8] Y. Q. Wang, J. W. Zu, Vibration behaviors of functionally graded rectangular plates with porosities and moving in thermal environment, Aerosp .Sci .Technol., 69 (2017) 550-562. https://doi.org/10.1016/j.ast.2017.07.023

[9] S. E. Sadiq, M. J. Jweeg, S. H. Bakhy, Strength analysis of aircraft sandwich structure with a honeycomb core: Theoretical and Experimental Approaches, Eng. Technol. J., 39 (2021) 153-166. https://doi.org/ 10.30684/etj.v39i1A.1722

[10] X. Wu, H. Yu, L. Guo, Li. Zhang, X. Sun, Z.Chai, Experimental and numerical investigation of static and fatigue behaviors of composites honeycomb sandwich structure, Compos. Struct., 213 (2019) 165–172. https://doi.org/10.1016/j.compstruct.2019.01.081

[11] E. K. Njim, M. Al-Waily, S. H. Bakhy, A Review of the Recent Research on the Experimental Tests of Functionally Graded Sandwich Panels, J. Mech. Eng. Res., 44 (2021) 420-441.

[12] L. Jing, X. Su, D. Chen, F. Yang, L. Zhao, Experimental and numerical study of sandwich beams with layered-gradient foam cores under low-velocity impact, Thin-Walled Struct., 135 (2019) 227-244. https://doi.org/10.1016/j.tws.2018.11.011

[13] Z. Huang, Y. Zhou, G. Hu, W. Deng, H. Gao, L. Sui, Flexural resistance and deformation behavior of CFRP-ULCC-steel sandwich composite structures, Compos. Struct., 257 (2021) 113080. https://doi.org/10.1016/j.compstruct.2020.113080

[14] M. Kazemi, Experimental analysis of sandwich composite beams under three-point bending with an emphasis on the layering effects of foam core, Structures, 29 (2021) 383-391. https://doi.org/10.1016/j.istruc.2020.11.048

[15] A. A. Daikh , A. M. Zenkour, Effect of porosity on the bending analysis of various functionally graded sandwich plates, Mater. Res. Express., 6 (2019).

[16] B.V Sankar, An elasticity solution for functionally graded beams, Compos .Sci .Technol, 61 (2001) 689–696. https://doi.org/10.1016/S0266-3538(01)00007-0

[17] Z. Zhong ,T. Yu, Analytical solution of a cantilever functionally graded beam, Compos. Sci .Technol, 67 (2007) 481–488. doi:10.1016/j.compscitech.2006.08.023

[18] Y. A. Kang , XF. Li, Bending of functionally graded cantilever beams with power-law non-linearity subjected to an end force, Int .J. Non. Linear. Mech., 44 (2009) 696–703. https://doi.org/10.1016/j.ijnonlinmec.2009.02.016

[19] N. Gupta , E. Woldesenbet, Microscopic Studies of Syntactic Foams Tested Under Three-Point Bending Conditions, Eng.Technol. Conf. Energy, 1 (2002) 147-152. https://doi.10.1115/etce2002/cmda-29069

[20] K. Ravi , S. Sankaran, Three-Point Bend Test Study in Syntactic Foam. Part III: Effects of Interface Modification on Strength and Fractographic Features, J. Appl. Polym. Sci., 98 (2005) 687-693.

[21] A. F. Avila, Failure mode investigation of sandwich beams with functionally graded core, Compos. Struct., 81 (2007) 323-330. https://doi.org/10.1016/j.compstruct.2006.08.030

[22] C. S. Karthikeyan, S. Sankaran, Kishore, Influence of chopped strand fibres on the flexural behavior of a syntactic foam core system, Polym. Int., 49 (2000) 158-162.

[23] C.S. Karthikeyan, S. Sankaran, Kishore, Investigation of bending modulus of fiber reinforced syntactic foams for sandwich and structural applications, Polym. Adv. Technol. , 18 (2007) 254-256.

[24] X. Wu, H. Yu, L. Guo, L. Zhang, X. Sun, Z. Chai, Experimental and numerical investigation of static and fatigue behaviors of composites honeycomb sandwich structure, Compos. Struct., 213 (2019) 165–172. https://doi.org/10.1016/j.compstruct.2019.01.081

[25] N. Gupta, E. Woldesenbet, Characterization of Flexural Properties of Syntactic Foam Core Sandwich Composites and Effect of Density Variation, J. Compos. Mater., 39 (2005) 2197-2212.

[26] J. Hohe, V. Hardenacke, V. Fascio, Y. Girard, J. Baumeister, K. Stöbener, J. Weise, D. Lehmhus, S. Pattofatto, H. Zeng, H. Zhao, V. Calbucci, F. Rustichelli, and F. Fiori, Numerical and experimental design of graded cellular sandwich cores for multifunctional aerospace applications, J. Mater. Des., 39 (2012) 20–32. https://doi.org/10.1016/j.matdes.2012.01.043

[27] A. Garg, H.D. Chalak, A. Chakrabarti, Comparative study on the bending of sandwich FGM beams made up of different material variation laws using refined layerwise theory, Mech. Mater., 151 (2020) 103634. https://doi.org/10.1016/j.mechmat.2020.103634

[28] L. Jing, X. Su, D. Chen, F. Yang, L. Zhao, Experimental and numerical study of sandwich beams with layered-gradient foam cores under low-velocity impact, Thin-Walled Struct., 135(2019) 227-244. https://doi.org/10.1016/j.tws.2018.11.011

[29] A. Seyedkanani, H. Niknam, A. H. Akbarzadeh, Bending behavior of optimally graded 3D printed cellular beams, Addit. Manuf., 35(2020) 101327. https://doi.org/10.1016/j.addma.2020.101327

[30] M. Bocciarelli, G. Bolzon, G. Maier, Three-Point-Bending and Indentation Tests for the Calibration of Functionally Graded Material Models by Inverse Analysis, In: Motasoares C.A. et al. (eds) III European , Conf. Comp.Mec. Spr. Dor., (2006).

[31] L. Czechowski, Study on Strength and Stiffness of WC-Co-NiCr Graded Samples, Mater., 12 (2019) 4166. https://doi.10.3390/ma12244166

[32] J. Zhou, Z.W. Guan, W.J. Cantwell, The impact response of graded foam sandwich structures, Compos. Struct., 97 (2013) 370–377. https://doi.org/10.1016/j.compstruct.2012.10.037

[33] S. Natarajan G. Manickam, Bending and vibration of functionally graded material sandwich plates using an accurate theory, Finite Elem. Anal. Des., 57 (2012) 32-42. https://doi.org/10.1016/j.finel.2012.03.006

[34] Sh. H. Hashemi , H. R. D. Taher, b. H. Akhavan , M. Omidi , Free Vibration of Functionally Graded Rectangular Plates Using First-Order Shear Deformation Plate Theory, Appl. Math. Model., 34 (2010) 1276-1291. https://doi.org/10.1016/j.apm.2009.08.008

[35] N. Wattanasakulpong, A. Chaikittiratana, Flexural vibration of imperfect functionally graded beams based on Timoshenko beam theory: Chebyshev collocation method, Mec., 50 (2015) 1331-1342. https://doi.org/10.1007/s11012-014-0094-8

[36] D. Lukkassen , A. Meidell, Advanced materials and structures and their fabrication processes, Book manuscript, Narvik University College, HiN., (2007).

[37] M. M. Hanon, R. Marczis, L. Zsidai, Influence of the 3D Printing Process Settings on Tensile Strength of PLA and HT-PLA, Period. Polytech. Mech. Eng., 65 (2021) 38–46. https://doi.10.3311/ppme.13683

[38] R. T. L. Ferreira, I. C. Amatte, T. A. Dutra, D. Bürger, Experimental characterization and micrograph of 3D printed PLA and PLA reinforced with short carbon fibers, Compos. Part B. Eng., 124 (2017) 88–100. https://doi.org/10.1016/j.compositesb.2017.05.013

[39] L. Wang, W. M. Gramlich, D. J. Gardner, Improving the impact strength of Poly(lactic acid) (PLA) in fused layer modeling (FLM), Polym. , 114 (2017) 242–248. https://doi.org/10.1016/j.polymer.2017.03.011

[40] A. Z. Mahdi, S. A. Amin, S. H. Bakhy, Influence of Refill Friction Stir Spot Welding Technique on the Mechanical Properties and Microstructure of Aluminum AA5052 and AA6061-T3, IOP. Conf. Ser. Mater. Sci. Eng., 671(2020).

[41] B. R. L. Yadhav, H.K. Govindaraju, M.D. Kiran, B. Suresha, Three-point bending and impact behavior of carbon/epoxy composites modified with titanium dioxide nanoparticles, Mater. Today. Proc., 43 (2021) 1755-1761., https://doi.org/10.1016/j.matpr.2020.10.442

[42] ASTM Standards, Standard Test Method for Flexural Properties of Sandwich Constructions, C 393 – 00,(2005).

[43] E. Sadiq, S. H. Bakhy, M. J. Jweeg, The Effects of Honeycomb Parameters on Transient Response of an Aircraft Sandwich Panel Structure, IOP Conf. Ser. Mater. Sci. Eng., 928 (2020) 22126. https://doi.org/10.1088/1757-899X/928/2/022126

[44] M. J. Jweeg, M. Al-Waily, A. K. Muhammad, K. K. Resan, Effects of Temperature on the Characterization of a New Design for a Non-Articulated Prosthetic Foot, IOP Conf. Ser. Mater. Sci. Eng, 433 (2018),

[45] S. Farah, D. G. Anderson, R. Langer, Physical and Mechanical Properties of PLA, and their functions in widespread applications-Acomprehensive Review, Adv. Drug Delivery Rev., 107 (2016) 367–392. https://doi.org/10.1016/j.addr.2016.06.012